Indian Journal of Fibre and Textile Engineering (IJFTE)
ISSN: 2582-936X (Online), Volume-2 Issue-2, November 2022

Optimization of Fabric Parameters on the Effectual Properties of Nonwoven Industrial Wipes Blend using Response Surface Methodology

Jonathan Tersur Orasugh, Kausik Bal, Dipankar Chattopadhyay, Swapan Kumar Ghosh, Suprakash Sinha Ray

Abstract*: *Development in technical in textiles especially nonwoven fabrics/materials offers a brightly limitless prospect for the textile industry to lance into an extensive series of applications ranging from earth to space and beyond. Nonwoven industrial wipes fabric properties are the result of production technology and the combination of fabric constructional parameters. This work looks into the effect of fabric parameters on the desired properties of nonwoven industrial wipes fabricated by needle punching technique with the utilization of viscose and polyester fibres and their blends using RSM. The basic and essential characterization techniques to obtain information related to physiochemical properties of the nonwoven fabrics, using analytical investigation techniques have been evaluated. The results obtained established that the fabric parameters have a great influence on the nonwoven fabric structure and ultimately its properties. The result revealed that higher content of PET fibres led to a reduction in the vertical wicking rate, but better rising height can be achieved at samples made from 100 % of viscose fibres. Also, the influence of pore size and porosity largely influenced the fabric characteristics. The fibre volume fraction on the strength of nonwovens has been studied. The fabricated wipes present themselves as potential candidates for highly absorbent industrial wipes.

Keywords*: *Textiles, Nonwovens, Bonding, Web formation, Consumer wipes, Industrial wipes, Market, Technology.

I. INTRODUCTION

The utilization of nonwovens has significantly augmented along with constant annual growth of 5–10% within the last decades [1,2]. Diverse nonwovens call for different fabric properties such as nature of polymeric material used for the fabrication of the fibres, fibre linear density, fibre shape, fibre surface roughness, and surface functions groups, fibre size/diameter, packing density, web pore size, fibre orientation angle (FOA) within the nonwoven, and so on. The aforementioned properties also influence the physical, mechanical and chemical performance like wicking rate, contact angle, mechanical strength, thermal and acoustic insulating properties, water/air permeability, barrier properties, etc. in the nonwoven fabric especially nonwoven industrial wipes (NIW). Summarily, NIWs properties are affected by the fibre, fabric, and other properties as depicted in Fig. 1. These properties, in turn, influence the fabric basic weight, packing density, porosity which in turn controls the properties and performance of the nonwovens. Whenever a nonwoven is intended for NIWs application, hydrophilic (cotton, viscose rayon, hydrophilic polyester, rayon, viscose, acetate and spun nylon, etc.), oleophilic (polyester, acrylic, modacrylic, polypropylene (PP) or polyethylene (PE), etc.) and other fibres are selected based on the fluid to be wiped/absorbed. The fluid absorbed subjugates the voids unoccupied by the fibres (i.e., the pores). This unoccupied void (porosity) in the NIW structure determines the amount of fluid absorbed. The fluid viscosity also influences the design and engineering of the NIW structure been a vital factor that affects the wicking rate/capillary force within the NIW fabric capable of storing and releasing the absorbed fluid.

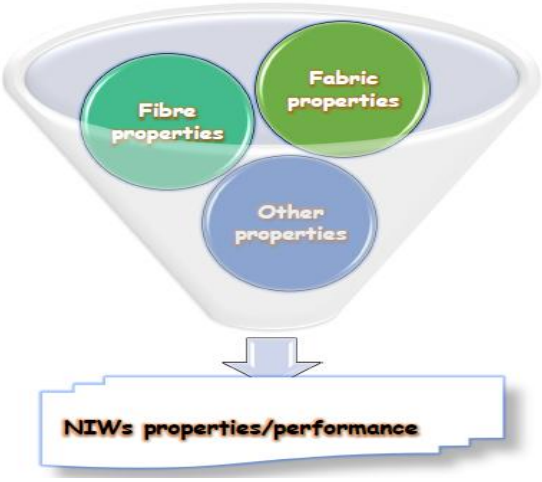

Fig. 1: Factors affecting the NIWs properties/performance

Manuscript received on 02 December 2021 | Revised Manuscript received on 22 July 2022 | Manuscript Accepted on 15 November 2022 | Manuscript published on 30 November 2022.
***Corresponding author (s) at:** Tel: +919831324354 | +919007734520 E-mail: ijtskg40@gmail.com | kbal.ucal@gmail.com | Fax: 033-24615632
Jonathan Tersur Orasugh[a,b,c,d,e], Kausik Bal[*b], Dipankar Chattopadhyay[a], Swapan Kumar Ghosh[*b], Suprakash Sinha Ray[c,d]
[a]Department of Polymer Science and Technology, University of Calcutta, 92 A.P.C. Road, Kolkata -700 009, India.
[b]Department of Jute and Fibre Technology, Institute of Jute Technology, University of Calcutta, 35 Ballygunge Circular Road, Kolkata -700 019, West Bengal, India.
[c]Department of Chemical Sciences, University of Johannesburg, Doorfontein, Johannesburg 2028, South Africa.
[d]DST-CSIR National Centre for Nanostructured Materials, Council for Scientific and Industrial Research, Pretoria 0001, South Africa.
[e]Department of Chemistry, University of Abuja, P.M.B 117 Main Campus, Abuja Airport Road FCT – Abuja, Nigeria.

Development in technical textiles especially nonwoven fabrics/materials offers a brightly limitless prospect for the textile industry to lance into an extensive series of applications ranging from earth to space and beyond.

Nonwovens are defined by ISO as structures of textile materials, such as fibres, continuous filaments, or chopped yarns of any nature or origin, that have been formed into webs by any means, and bonded together by any means, excluding the interlacing of yarns as in woven fabric, knitted fabric, laces, braided fabric or tufted fabric [1]. At the onset, nonwovens were used conventionally in medical textiles: conversely, nonwovens have within the last decades made an outstanding impact in new areas such as industrial wipes.

One of the prime benefits offered by NIWs/IWs is expediency; using a wipe is speedier and easier in comparison to conventional methods of dispensing a liquid and then using a second cloth/towel to clean or eliminate the liquid: industrial wipes particularly prewetted wipes do both of the aforementioned processes without the need for a solvent/liquid. Multilayer and blend engineered IWs have reportedly been shown to absorb more water and oil than orthodox rags and stay strong for superior performance and the disposable cloths clean oil, dirt, grime, and solvents while remaining resistant to harsh cleaning agents [3,4]. IWs (categorized as disposable and semi-durable wipes) are produced from woven, nonwovens, nonwoven composites and flock fibres, etc. [3,4]. There are reports on the study on several properties of wipes for diverse applications in literature [3,4,5]. This paper presents a study on the effect of fabric/processing parameters on the properties of novel engineered nonwoven virgin polyester, viscose and their blends such as porosity, pore volume/size, bending rigidity, abrasion resistance, surface properties, wetting, wicking rate, compressional properties, and surface morphology properties using response surface methodology optimization approach. The consideration of such blends for IWs applications has not been reported nor studied up to date. The fabrication of nonwoven IWs (NIWs) using a blend of nontoxic hydrophilic fibres for hygiene products is regarded by its excellence in demand on the products. Looking at the industrial-consumer end of the NIWs market, the principal trend has been efforts by manufacturers to upsurge the market portion occupied by eco-friendly NIWs above competitors producing non-eco-friendly rags or rental shop towels: our drive is to present an eco-friendly material via facile approach for the fabrication and potential application of polymer fibre blend NIWs under optimized conditions.

II. MATERIALS AND METHODS

The materials used in this work are polyester and viscose rayon fibres. The fibres were used to fabricate a number of nonwovens as presented in Table 1. All NIW samples were conditioned as specified by standard atmospheric conditions of 21 ± 1°C and 65 ± 2% relative humidity within a period of ~24 h before commencing testing.

Table 1: Features of wipes adopted.

Sample	Composition	Thickness (mm)	GSM	Average pore size (μm)
P10	PET100	0.624±0.046	59.6±0.37	16.144
V10	VES100	1.632±0.099	122.2±0.59	7.702
V6P4	VES60PET40	1.976±0.042	121±0.11	18.247
V7P4	VES70PET30	1.878±0.053	113.4±0.44	16.131

2.1. Characterization

2.1.1. Scanning electron microscopy (SEM)

The surface morphology of all the samples was observed using a ZEISS EVO 18 scanning electron microscope (SEM). The samples were gold-coated before it was mounted on the sample holder of the SEM. The acceleration voltage was set at 15 kV and a distance of 8 mm. The diameter of the samples was determined directly from the SEM images. The average pore size (μm) and area (μm^2) of the specimens were evaluated via *ImageJ* software.

2.1.2. Mass per unit area analysis

The mass of the samples per unit area (g/m^2) was estimated using ISO 9073-1: 1989, DIN EN 29073/DIN EN 1227 (NWSP 130.1.R0 (15)) or WSP 130.1, ASTM D3776/ D3776M-09a(2017), etc. The analysis was executed by weighing the sample having dimensions (m) as specified in the aforementioned standard and then the weight (g) was divided by the area (m^2) of the sample to get the mass per unit area also known as GSM.

2.1.3. Sample thickness analysis

The average thickness of the IWs was measured following DIN EN ISO 5084, ISO 9073-2: 1995 (NWSP 120.6.R0 (15)), ASTM D1777 - 96(2019), with the help of a thickness gauge (analogue/digital in mm) by subjecting the test specimen to a predetermined pressure between two plane-parallel plates. The distance between the plates was recorded as the thickness of the specimens.

2.1.4. Measurement of NIW vertical wicking rate

The vertical wicking rates of the IWs samples were tested according to DIN 53924 by measuring the wicking height against gravity along the longitudinal direction of the specimen. Five IW strips for each sample having dimension of 200×25 mm, with a 10 mm distance line mark from the lower edge of the strip were preconditioned for 24 hours in a standard testing atmosphere of 20±2 °C and 65±2 % of relative humidity (ISO 139:2005(E)). Each tested sample was suspended vertically with its bottom ends at an immersion depth into a methylene blue solution along with the activation of the stopwatch at the same time (Fig. 2). The rising capillary/wicking height was recorded, and the average value was determined and considered as the final result.

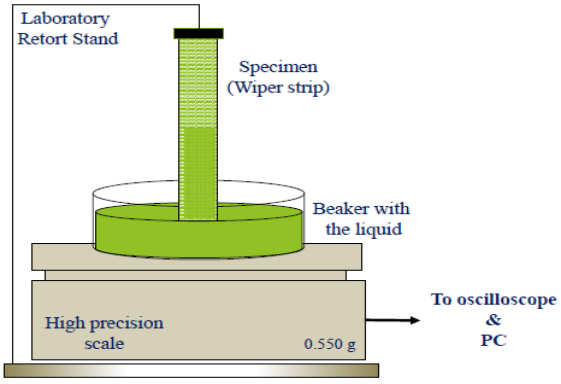

Fig. 2: Scheme: capillary liquid absorption (vertical wicking rate) of cleaning wipers

2.1.5. Process optimization for VWR using RSM

Optimization of the VWR adsorption the NIWs was carried out with a three-factor three-level central composite design model designed by the central composite design (CCD) feature of RSM using Design Expert (Version 7.0 Minneapolis, USA). The selected process variables include fibre density, porosity, and GSM. The VWR of the NIWs was carefully chosen as the *output* response and estimated from the experiments comprising six repetitions at the central point as suggested by this model.

The experiment collection, levels of the independent variables, and experiments commended by the RSM (CCD) is shown in Table S1, S2, S3, and S4. The influence of the inter-parameter relations on the chosen process as shown in this study is depicted as 3D plots Fig 10, 11, 12, and 13 which were also utilized for the determination of the optimum conditions enabling maximum process proficiency. The experiments were in triplicate repeated and the mean values were taken for the final data examination. The empirical relationship of the three chosen independent variables in this study is determined using the quadratic polynomial equation as shown below:

$$Y = m_0 + \sum_{i=1}^{k=3} m_i x_i + \sum_{i=1}^{k=3}\sum_{j=1}^{k=3} m_{ij} x_i x_j + \sum_{i=1}^{k=3} m_{ii} x_i^2 + e \quad \ldots. (i)$$

Where, Y represents dependent variable(response), $m_0$is the constant coefficient, $m_\alpha(\alpha = i,j,ij)$ is the regression coefficients of linear, quadratic and interaction models respectively, $x_\alpha(\alpha = i,j)$ represents the experimental parameters (independent variables) and e denotes the error. The optimized experimental conditions for guaranteeing maximum effectiveness of the process governed using Derringer's desirability function [6].

2.1.6. Moisture absorption (MA) and moisture content analysis

The moisture absorption and moisture content were determined according to NWSP 230.0.R2 (15) ISO 17190-4:2001. Three samples were dried to a constant weight (W_1) in a vacuum oven at 80 – 100 °C. The NIW samples were then kept in a 75% constant R.H atmosphere fashioned with the help of hermetic glass desiccators containing saturated $CaCl_2$ solution.

The weight (W_2) of all the samples was considered after 24 h. M.A of specimens was determined by adopting equation (*ii*) [7,8]. Again, the M.C of the specimens was estimated by drying the samples to a constant weight (W_1) in a vacuum oven at 80 -100 °C and kept in a constant humidity chamber (desiccators) containing activated silica for 24 hours. The weight of each sample was repeatedly weighed until an equilibrium weight was attained. The percentage of moisture content has been calculated using the following equation (*iii*).

$$\text{Moisture absorption (\%)} = [(w_2 - w_1)/w_1] \times 100 \quad (ii)$$

$$\text{Moisture content (\%)} = [(w_1 - w_2)/w_2] \times 100 \quad (iii)$$

3.1.7. Packing density and porosity analysis

The packing density of NIWs can be determined from the GSM (fabric basis weight), the fabric thickness, and the fibre density. The porosity (ε) of NIW presents information about the entire pore volume of the porous material. NIW ε is referred to as the ratio of the non-solid volume or voids to the entire volume of NIW fabric. Also, the packing density/volume fraction of solid material is referred to as the ratio of fibre density/volume to the overall density/volume of fabric. Knowing that the density of the NIW fibre is the weight of a given volume of the solid fibre; its ε is calculated as shown in equation (*iv*) – (*v*). From the measured NIWs GSM and thickness, the porosity was determined via the following expressions:

$$\phi = V_{fib}/V_{fab} = (W_{fib}/\rho_{fib})/t_{fab} = \text{Basic weight}/t_{fab}x\rho_{fib} \quad (iv)$$

$$\phi\ (\%) = (\rho_{fab}/\rho_{fib})100 \quad (v)$$

$$\rho_{fab}(kgm^{-3}) = W_f/t\ (kgm^{-3}) \quad (vi)$$

Where V_{fib} = volume of fibers m^3; V_{fab} = volume of the fabric m^3; W_{fib} = weight of fibers = weight of the fabric (gm^{-2}); ρ_{fib} = NIW fiber or polymer density kgm^{-3}; t_{fab} = thickness of the NIW fabric; and A = area of the web (m^2).

Porosity (ε) is the fraction of the void volume to the volume of the web, i.e.:

$$\varepsilon\ (\%) = (1 - \phi)100\% \quad (vii)$$

Here, ε is the NIW porosity (%), ϕ is the packing density/volume fraction of solid material (%), ρ_{fab} (kgm^{-3}) is the bulk density of NIW fabric and ρ_{fib} (kgm^{-3}) is the density of fibre.

Porosity, pore size, and pore size distribution: The pore structure in NIWs encompasses the total pore volume or porosity, the pore size, pore size distribution, along with connectivity of the pores.

2.1.8. Fibre orientation distribution (FOD) analysis

NIWs fibres are alignment in nonwoven structures in various paths. The alignment of these fibres is inherent properties from alignments of fibres in the nonwoven fibrous webs and fibre rearrangement in the bonding process of the nonwovens such as in needle punching, hydro-entanglement, etc. This property can be defined by fibre orientation angles (FOA) in 2D or 3D as depicted in Fig. 3.

In nonwovens like NIWs, the orientations of fibres in such structures are hypothetically or even practically in any of direction of the 3D having a complex fibre alignment resulting in high-cost of measurement [9]. It is important to note that a large proportion of the fibres within the NIWs are oriented in the MD or approximately CD.

Consequently, the nonwoven fabric 3D structure often results in an amalgamation of numerous strata's of 2D structures having fibres in the transverse direction to the MD or fabric plane as depicted in Fig. 3.

Hence, the fibre orientation in 3D NIWs can be defined by the fibre alignments in 2D like the fibre orientation in NIWs MD where fibre orientation is described by the fibre orientation angle. (FOA) being a representation of the relative directional locus of singular fibres in the NIWs or nonwoven structure, typically relative to the CD/MD as presented in Fig. 3. FOA of the fabricated NIW's distinct fibres were evaluated by analyzing the nonwoven web or NIWs micrographs/images and image analysis software's [10,11,12,13]. The FOA of the NIW samples was determined using the SEM micrographs obtained from SEM (ZEISS EVO-MA10, Germany).

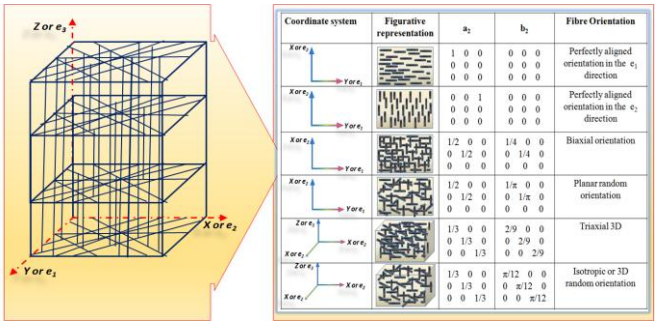

Fig. 3: Fibre orientation angle in 2D and 3D nonwoven fabrics.

2.1.9. Bursting strength

The Diaphragm Bursting Strength Test Method according ASTM-D3786-089 (corresponding to NWSP 030.1.R0 (15), NWSP 030.2.R0 (15), ISO 13938-1:1999 and ISO 13938-2:1999) was adopted to characterize the NIWs. The sample was clamped over an expandable diaphragm where the diaphragm was expanded via fluid pressure until the rupture of the specimen. The difference between the overall pressure obligatory to rupture the specimen and the pressure requisite for inflation of the diaphragm is considered as the bursting strength.

2.1.10. Air and water permeability

Intrinsic fluid (air, water, etc.) permeability also referred to as absolute or specific permeability of NIWs or nonwovens relies exclusively on the structure of these fabrics and signifies the void capacity the fluid is able to flow through. In real-life use of nonwoven fabrics for technical applications like wipers, geotextiles, etc. the preferred parameter is the use of permeability coefficient, K (m/s), which is also referred to as Darcy's constant/coefficient or conductivity. The relationship between k and K is represented by: $k=K\eta/\rho g$ (m^2), where ρ is the density of the liquid (kg/m^3), and g is the accelerator due to gravity (m/s^2). The value of the constant k (m^2) is 1.042 x $10^{-7}K$ (m/s) for water at 20°C. In this work the permeability was determined following ASTM D737-96; BS EN ISO 9237:1995; ISO/DIS 9073-15: 2005; WSP 70.1-05.

2.1.11. Drop penetration time (DPT)

Liquid (mostly water or other liquids) drop penetration time (DPT) gives researchers the idea of how long it takes for the fluid to completely penetrate through the NIW via absorption mechanism. A DPT result makes it feasible to gain insight into the dynamics of the liquid absorption of NIW especially in NIWs made from hydrophobic fibres for evaluation of the effectiveness of the chemical hydrophilisation unto application. The DPT was carried out by photographing the drop penetration process with a high-speed digital camera and the imaging sequences were collected with an accurate time stamp (in 1/1000 s), aimed at determining the time period between the liquid drop contact with the NIWs surface and its complete penetration through the NIW. The drop is considered to be completely submerged as soon as there is no longer any reflection due to the liquid visible on the NIW. The test setup was fixed on an optical bench which enabled the sliding of individual parts - the camera (250 images/sec), the sample holder, and the translucent glass screen - along the optical axis. The translucent glass screen was illuminated from behind by a split ring light. The surface of the samples was occasionally illuminated as the need arise by a swan neck light conductor. The liquid drops were applied with a motorized precision pipette attached to the equipment. The time between drop impact and complete penetration was calculated and recorded. However, due to the non-availability of the instrument arising from the Covid-19 lockdown in colleges and universities, this experiment was performed manually using an acupipette and a stopwatch. 0.2 ml of H_2O was poured on the NIW with immediate activation of the stopwatch. The time taken for the drop submerges was noted as the drop penetration time and recorded: this experiment was performed five times and the average value was taken.

III. RESULTS AND DISCUSSION

3.1. Scanning electron microscopy (SEM)

The scanning electron microscopy images showing the morphology of the NIW samples are depicted in Fig. 4. The samples (Fig. 4a,b,c,d (i-ii)) reveal a dense fibrous surface properties for P10, V10, V6P4, and V7P4 while Fig. 4a,b,c,d (iii) represents the *ImageJ* pore size outline. The mean pore size of P10, V10, V60P40, and V70P30 as calculated using the *ImageJ* software was found to be 16.144, 7.702, 18.247, 16.131 µm respectively.

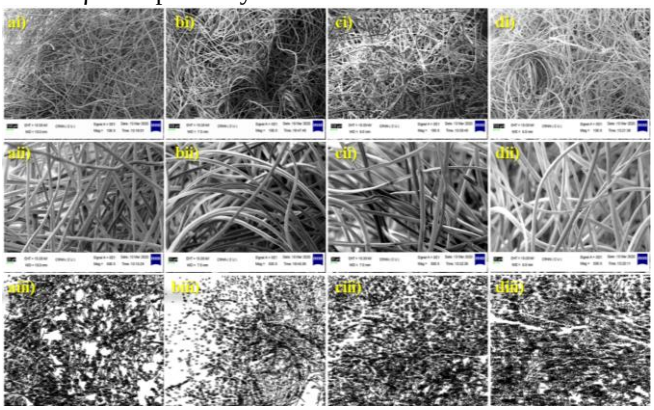

Fig. 4: SEM micrographs showing a) PET, b) VES, c) V6P4, and d) V7P4's surface morphology (i-ii) and ImageJ pore size outline (iii).

3.2. Mass per unit area analysis

The mass per unit area which is also referred to as GSM of P10, V10, V60P40, and V70P30 as calculated as per ISO 9073-1: 1989 is 59.6 ± 0.37, 122.2 ± 0.59, 121.0 ± 0.11, and 113.4 ± 0.44 g/m^2 respectively and also shown in Table 1 & 2 and Fig. 8. Characteristically, the uniformity of the NIW fabric is referred to as the CV. The CV value for P10, V10, V60P40, and V70P30 as calculated from NIWs GSM is 4.83, 5.32, 1.01, and 4.16 % respectively. Also, as depicted in Fig. 8, the GSM of all the NIWs showing a direct relationship to the bursting strength and vice versa.

3.3. Sample thickness

The thickness of the samples "P10, V10, V60P40, and V70P30" (Fig. 8d) as determined using ASTM D1777 - 96(2019) is 0.0624, 0.1632, 0.1976, 0.1878 cm respectively, and also shown in Table 1. CV of P10, V10, V60P40, and V70P30 is 4.62, 9.86, 4.21, and 5.34 %. As presented in.

Table. 2, the thickness of the sample revealed a direct relationship to the bursting strength and vice versa.

3.4. Fabric Vertical Wicking Rate of NIWs

Porosity vs. Vertical Wicking Rate: The vertical wicking rate results are presented in Table 2. Fig. 9 depicts the influence of porosity on the vertical wicking rate and the fibre composition of the NIWs because more air trapped within the pores in the structure of the fabric, allows more rapidly movement of water through the pores. The structural porosity of the NIWs is a property of the result of their fabrication/processing parameters. It is observed from Fig. 9 that the higher the porosity, the higher the vertical wicking rate of the NIWs. Also, the fibre content of the NIWs (hydrophilic/hydrophobic fibres) has a great influence on the wicking rate. With the analysis of the samples' porosity structure with respect to the composition of VIS/PES fibres via the pore size distribution (Fig. 9), it was observed that the samples with higher porosity demonstrated higher average pore diameter/size (see also Table 2). The NIWs having larger pores revealed a higher wicking rate which agrees well with capillarity theory: fluid flow is faster in a void with a large capillary radius in comparison to voids with a smaller radius. This implies that the fluid (water) travels from the bigger pores to the minor pores as the height upsurges. However, looking at the results with regards to the blends having the content of viscose and polyester fibres in the web, the results are somewhat confusing and require careful interpretation. For instance, in the blends: higher content of viscose fibres showed improved vertical wicking rate, which is indicative of the higher absorption rate of viscose fibres leading to assisted capillary action/VWR and consequently enhanced movement of water through the pores at a faster rate. Our findings are in the consonance with previous literature [3,9,14]. Then again, samples of NIWs having 100 % of polyester fibres presented results very close but less than those made from 100% viscose fibres. This calls for the necessity of a predictive tool such as a predictive model effective study of the fabric parameters and how they relate to the porosity and the VWR of the NIWs.

Table 2: NIWs GSM, Packing density, porosity, and wicking rate results

Sample	ρ_{fib}(g/cm^3)	GSM (g/m^2)	Web thickness (cm)	Bursting strength (N)	Packing density	Porosity (%)	Experimental VWR (mm)
P10 (MD)	1.38	59.6 ± 0.37	0.0624 ± 0.046	5.0±0.14	0.069	93.08	35 ± 1.05
P10 (CD)				5.2±0.07			38 ± 1.14
V10 (MD)	1.53	122.2 ± 0.59	0.1632 ± 0.099	7.8±0.02	0.049	95.11	37 ± 1.11
V10 (CD)				7.9±0.12			41 ± 1.23
V6P4 (MD)	1.47	121 ± 0.11	0.1976 ± 0.042	7.8±0.06	0.042	95.83	20 ± 0.60
V6P4 (CD)				7.9±0.07			23 ± 0.69
V7P3 (MD)	1.49	113.4 ± 0.44	0.1878 ± 0.053	7.4±0.05	0.041	95.95	23 ± 0.69
V7P3 (CD)				7.4±0.06			30 ± 0.90

3.5. Moisture absorption (MA) and moisture content (MC)

The *MA* of the samples "P10, V10, V60P40, and V70P30" as determined following international standards was found to be 9.02, 22.76, 7.02, and 7.28 % respectively, as also shown in Fig. 5a. Also, the *MC* of the NIWs "P10, V10, V60P40, and V70P30" was found to be 6.51, 12.46, 5.50, and 8.90 % respectively, as also depicted in Fig. 5b.

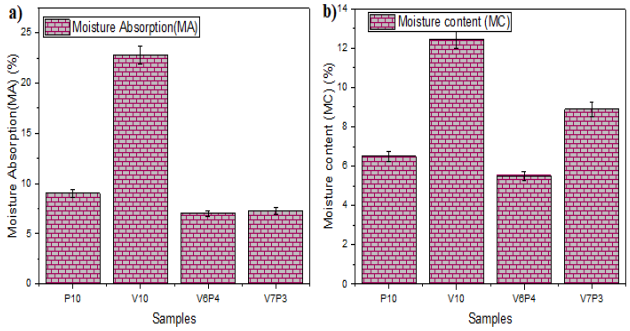

Fig. 5: MA (a) and MC (b) of P10, V10, V6P4, and V7P3

3.6. Porosity, pore size, and pore size distribution

The porosity of the samples: "P10, V10, V60P40, and V70P30" (Fig. 6a) was determined and found to be 93.08, 95.11, 95.83, and 95.95 % respectively. The porosity of the samples showed a direct relationship with the VWR. This result is supported by previous literature [15,16,17]. The average pore sizes of the NIWs; P10, V10, V60P40, and V70P30 determined using *ImageJ* as represented in Fig. 6b are 16.144, 7.702, 18.247, and 16.131 μm respectively. Also, the *pore size distribution* of the "P10, V10, V60P40, and V70P30" estimated from *ImageJ* is depicted in Fig. 6c.

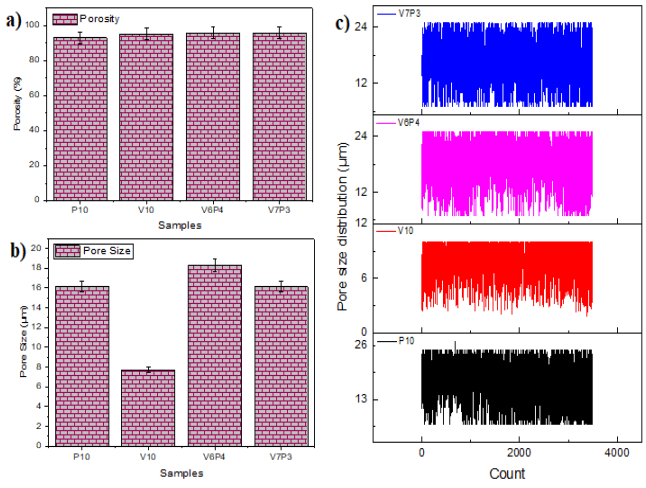

Fig. 6: Porosity (a), Pore size (b), and pore size distribution of P10, V10, V6P4, and V7P3

3.7. Fibre orientation distribution

The FOA of the nonwoven industrial wipes for "P10, V10, V60P40, and V70P30" (Fig. 7a) was determined using *ImageJ* software and found to be 69.861, 65.274, 63.533, and 65.029° respectively. The FOD as shown in Fig. 7b reveals a direct relationship to the bursting strength which is in agreement with previous reports [18].

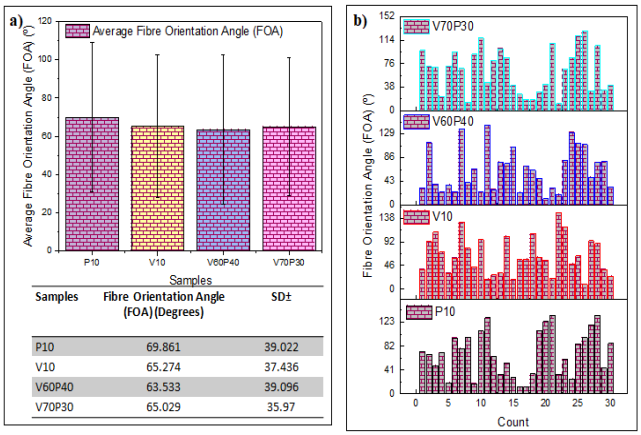

Samples	Fibre Orientation Angle (FOA) (Degrees)	SD±
P10	69.861	39.022
V10	65.274	37.436
V60P40	63.533	39.096
V70P30	65.029	35.97

Fig. 7: a) The FOA, and b) FOD of P10, V10, V6P4, and V7P3 NIWs

3.8. Bursting strength

The bursting strength of NIWs defines the force applied at right angles to the fabric plane under predetermined conditions resulting in the rupture of the nonwoven fabric [19,20,21,22]. The BSs of NIW samples are presented and depicted in Table 2 and Fig. 8. The bursting strength showed a direct relationship to the thickness of the fabrics which agrees with previous literature [19,20,21,22]. However, there is a need for the adoption of effective and efficient prediction software tools to ascertain the optimized bursting strength with respect to corresponding fabric thickness.

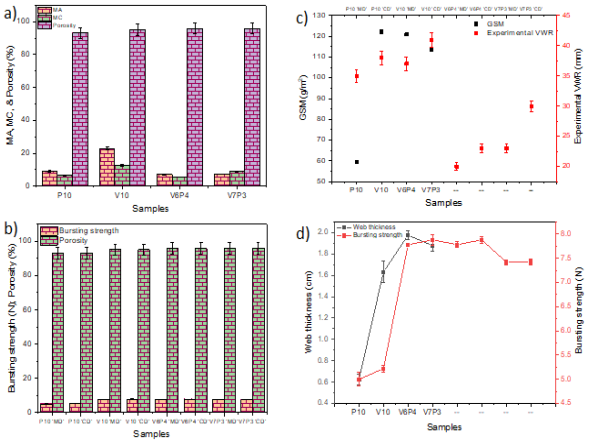

Fig. 8: a) Bursting strength (BS), b) BS vs web thickness, c) BS vs GSM, d) BS vs porosity of P10, V10, V6P4, and V7P3 NIWs

3.9. Air and water permeability

The dimensions of the fabric as well as yarn pores, and other material and structural aspects of a fabric, such as the weave, the source material of the fibres or yarns, the set of yarns, and others, all have a significant impact on how permeable a fabric is to air. The air permeability of P10, V10, V60P40, and V70P30 as determined as per ASTM D737-96 was found to be 437912.42, 254949.01, 332933.41, and 371925.61$cm^3/s/cm^2$ respectively. It was observed that the thickness, packing density, pore size, and porosity have a great influence on the air permeability of the respective NIW samples even as reported in the literature [16,17,23]. The air permeability of all the NIWs was measured at a constant pressure head of 300 Pa. Several fabric end-uses, such as industrial wipes, filters, tents, sailcloths, parachutes, raincoat materials, shirtings, down-proof fabrics, airbags, and so forth, require comfort in addition to clothing.

3.10. Drop penetration time (DPT)

The DPT of the NIWs (as in Fig. 9; Table 3): "P10, V10, V60P40, and V70P30" is 0.42, 0.10, 0.3, and 0.38 sec. respectively. The DPT reveals a direct relationship to the hydrophilic nature of the NIWs and to some extent, the pore size and GSM. The increase in the percentage of viscose fibres in the blend revealed a corresponding increase in the DPT as seen in Fig. 9. This result is in agreement with the VWR trend.

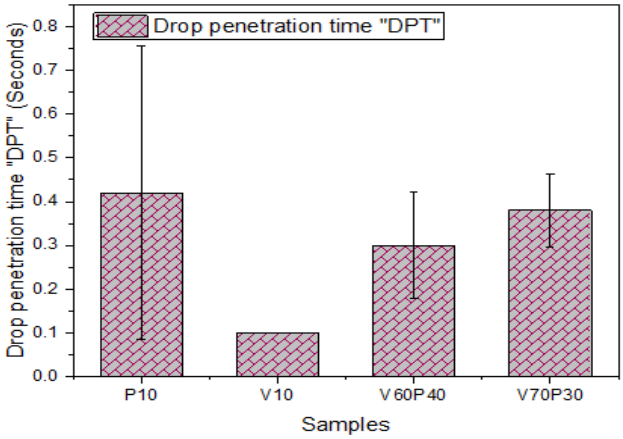

Fig. 9: Drop penetration time (DPT) for the fabricated NIWs

Table 3: Drop penetration time (DPT) for the fabricated NIWs

Samples	Average DPT (Sec.)	SD
V10	0.10	0
P10	0.42	0.33
V60P40	0.3	0.12
V70P30	0.38	0.08

3.11. RSM study for NIWs

The result of the vertical wicking rate (in mm) experiments performed using the CCD system is presented in Table S1, S2, S3, and S4 respectively. The model F values for the VWR were obtained from the Annova for response surface models. The predicted models for VWR presented the best fit along with a high significance with. F value for V10, P10, V60P40, and V70P30 are 69.56124374 (P<0.0001), 44.70127807 (P<0.0001), 34.48448923 (P<0.0001), and 124.8755118 (P<0.0001). This result proposes that there is only a 0.01 % chance that a large model F-value could occur due to the noise [24], while the "Lack of Fit F-value" was found to be highly insignificant. The regression coefficients have been found to be high and in realistic consensus with R^2; adjusted R^2; and predicted R^2 values for. V10, P10, V60P40, and V70P30 found to be 0.960863, 0.947049, and 0.923308; 0.973386, 0.95161, and 0.952765; 0.956838, 0.929091, and 0.907398; and 0.987696, 0.979787, and 0.965634 respectively. The predicted R^2 is in realistic bargain with the adjusted R^2 even as the value C.V. % for V10, P10, V60P40, and V70P30 been 0.378641815, 1.042457577, 1.224066668,

and 0.87275694 implies a good exactness and dependability of the experimental values. Hence, it has been concluded that the predicted model best describes the VWR for V10, P10, V60P40, and V70P30 as presented in equations (*viii*), (*ix*), (*x*), and (*xi*) respectively:

Vertical wicking rate (VWR) = -13924.41208 - 99.265804 * Fibre density + 154.9837123 * Porosity + 108.9272192 * GSM -4.349405002 * Fibre density * Porosity + 4.228714168 * Fibre density * GSM -1.212786189 * Porosity * GSM ……..(*viii*)

Vertical wicking rate (VWR) = -941.1480367 + 1110.921742 * Fibre density - 0.474437496 * Porosity + 9.140001914 * GSM - 7.946396448 * Fibre density * Porosity - 4.093721485 * Fibre density * GSM + 0.091657298 * Porosity * GSM - 54.46052523 * Fibre density^2 + 0.030667977 * Porosity^2 - 0.104518658 * GSM^2 ……..(*ix*)

Vertical wicking rate (VWR) = 1369370.037 + 8373.004426 * Fibre density + 1373.687887 * Porosity - 23827.60367 * GSM - 11.61654173 * Fibre density * Porosity - 60.83828397 * Fibre density * GSM - 11.03917445 * Porosity * GSM + 36.10135306 * Fibre density^2 - 0.111045446 * Porosity^2 + 103.2201307 * GSM^2 ……..(*x*)

Vertical wicking rate (VWR) = -13723.95387 + 4080.775026 * Fibre density + 11.13094751 * Porosity + 177.9945471 * GSM - 2.907066122 * Fibre density * Porosity - 0.407156039 * Fibre density * GSM - 0.043200333 * Porosity * GSM - 1225.755178 * Fibre density^2 -0.009161866 * Porosity^2 - 0.763770753 * GSM^2 ……(*xi*)

The predicted VWR of the NIWs deliberate using the aforementioned equations is also represented in Table S1, S2, S3, and S4 respectively together with its equivalent experimentally documented values. The results indicated a close match between the predicted values and the experimentally acquired results. Noteworthy inter-parameter interfaces and their mutual effect on the VWR of NIWs have been deliberated.

3.12. Optimization of the VWR process by desirability function

Fig. 10d; Fig. 11d; Fig. 12d; and Fig. 13d depict the predicted vs. actual VWR of the NIWs. With respect to the Derringer's desirability function (DF) having high desirability of 0.921, our optimized process conditions managing process proficiency was establish for V10; P10; V60P40; and V70P30 as 1.5766 g/cm^3, 95.23624%, and 122.2474 g/m^2; 1.305g/cm^3, 92.5%, and 58.4931828 g/m^2; 1.4708 g/cm^3, 95.87996%, and 120.9934 g/m^2; and 1.5356 g/cm^3, 95.33%, and 113.3936 g/m^2 respectively for the fibre density, porosity and GSM. Under the aforementioned optimized conditions, the response in terms of VWR of V10; P10; V60P40; and V70P30 was noted as 37.5, 34.33636364, 21.92, and 26.99 mm respectively, which is found to be in good comparison to the experimental results acquired from the batch study. The WVP properties of the studied materials is believed to be influenced by the porosity of the material as well as the fibre type used herewith.

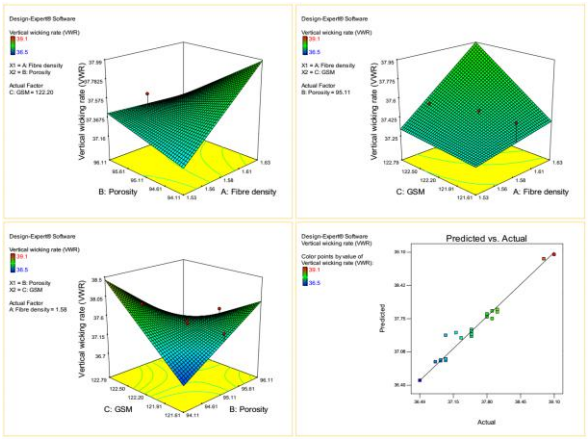

Fig. 10: (a-c) 3-D surface plots showcasing the interaction of different process parameters during the VWR a) Effect of porosity versus fibre density; b) Effect of GSM versus fibre density; and c) Effect of GSM versus porosity. d) Graph showing predicted VWR versus actual VWR of V10.

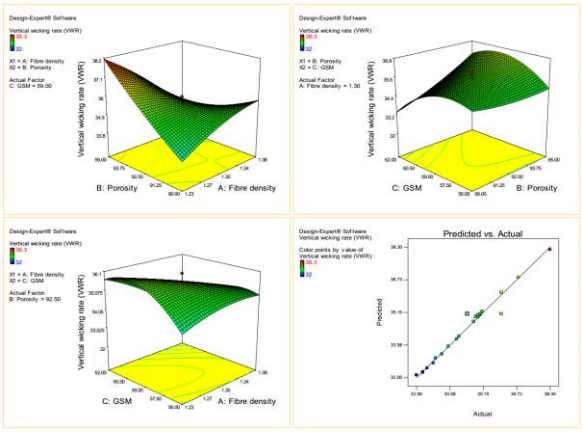

Fig. 11: (a-c) 3-D surface plots showcasing the interaction of different process parameters during the VWR a) Effect of porosity versus fibre density; b) Effect of GSM versus fibre density; and c) Effect of GSM versus porosity. d) Graph showing predicted VWR versus actual VWR of P10.

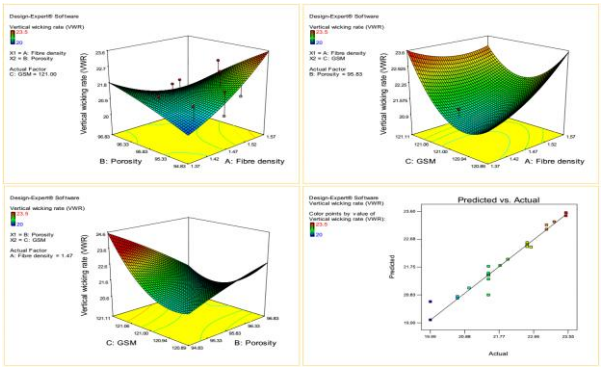

Fig. 12: (a-c) 3-D surface plots showcasing the interaction of different process parameters during the VWR a) Effect of porosity versus fibre density; b) Effect of GSM versus fibre density; and c) Effect of GSM versus porosity. d) Graph showing predicted VWR versus actual VWR of V60P40.

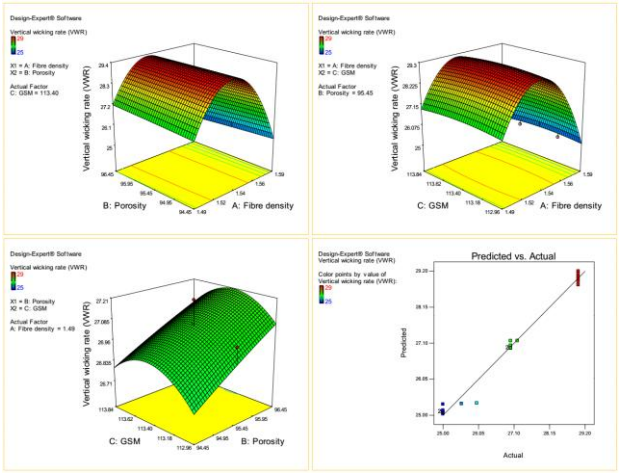

Fig. 13: (a-c) 3-D surface plots showcasing the interaction of different process parameters during the VWR a) Effect of porosity versus fibre density; b) Effect of GSM versus fibre density; and c) Effect of GSM versus porosity. d) Graph showing predicted VWR versus actual VWR of V70P30.

IV. CONCLUSION

In this study, NIWs samples of polyester fibres and viscose fibres varying in viscose/polyester ratio to determine their effect on the wicking rates. Potential NIWs were prepared from polyester and viscose fibres using needing punching technology. The effect of the fibre and fabric properties on the vertical wicking rate and other fabric properties have been carefully studied. The air permeability of the nonwoven industrial wipe samples showed dependence on the porosity. The bursting strength also reveals an inverse relationship with respect to the NIWs porosity and thickness. After statistically evaluating the data, the results have been summarized thus:

VWR is established to be significantly influenced by the porosity of the NIWs due to the fact that increase in porosity results in the formation of added passages for the fluid; the wicking rate ascertained to be influenced by the number of fibres intersections per unit density acting as transmitting channels for the fluid. Overall, the prepared NIWs presented a result suitable for application in wiping purposes.

ACKNOWLEDGMENTS

The authors wish to appreciate the Centre for Research in Nanoscience and Nanotechnology, Department of Polymer Science and Technology and the Department of Jute and Fibre Technology, Institute of Jute Technology, the University of Calcutta for and the University Grant Commission (UGC), Govt. of India for their financial and technical support

CREDIT AUTHOR STATEMENT

Prof. (Dr.) Swapan Kumar Ghosh who is the corresponding author is responsible for ensuring that the descriptions are accurate and agreed by all authors.

The role(s) of all authors are listed below:

Jonathan Tersur Orasugh: Is the original owner and initiator of this research work as guided by Prof. (Dr.) Swapan Kumar Gosh and Dr. Kausik Bal. He has overseen and partaken in every aspect of this article along with the research work, data interpretation, typing, editing, revision, formatting, submission, etc.

Kausik Bal: Helped with initiation of this work, assisted, and supported the authors in the arrangement and editing of the article. He is also a corresponding author to this article.

Prof. Dipankar Chattopadhyay: Was responsible for data interpretation, editing the review of this article.

Prof. (Dr.) Swapan Kumar Ghosh: Is the corresponding author and responsible for initiation of this research, guidance, editing, ensuring that the descriptions in the manuscript are accurate and agreed by all authors along with the communication of this article.

Prof. Suprakash Sinha Ray: Was responsible for editing the review of this article.

REFERENCES

1. N. Mao, S. J. Russell. (2015). In book: Textiles and Fashion: Fibre to Fabric. *Textiles and Fashion*, 307–335. doi:10.1016/b978-1-84569-931-4.00013-1. [CrossRef]
2. V. Edwards, P. Sawhney, A. Bopp, A. French, R. Slopek, M. Reynolds, … Montalvo, J. (2015). An Assessment of Surface Properties and Moisture Uptake of Nonwoven Fabrics from Ginning By-products. Cellulose - *Fundamental Aspects and Current Trends*. doi:10.5772/61329. [CrossRef]
3. V. Soukupova, L. Boguslavsky, D. R. AnandJiwala. (2007). Studies on the Properties of Biodegradable Wipes made by the Hydroentanglement Bonding Technique. *Textile Research Journal*, 77(5), 301–311. [CrossRef]
4. A. Watzl, J. Eisenacher, B. D. Gillespie. Nonwoven & Lifestyle – Spunlaced and Airlaid Nonwovens for Medical –Surgical – Health Care – Personal Care – Hygiene, in Proc.2001 Beltwide Cotton Conference, National Cotton Councilof America, Memphis, TN, USA, 698–701.
5. C. R. Frederic. (2004). Battle of Industrial Wipes, *Nonwoven Industry*, 56–65.
6. G. Derringer, R. Suich. (1980). Simultaneous optimization of several response variables. *Journal of Quality Technology*, 12(4), 214-219. [CrossRef]
7. J. T. Orasugh, N. R. Saha, G. Sarkar, D. Rana, R. Mishra, D. Mondal, S. K. Ghosh, D. Chattopadhyay. (2018a). Synthesis of methylcellulose/cellulose nano-crystals nanocomposites: Material properties and study of sustained release of ketorolac tromethamine. *Carbohydrate Polymers*, 188, 168-180. [CrossRef]
8. J. T. Orasugh, N. R. Saha, D. Rana, G. Sarkar, M. M. R. Mollick, A. Chattopadhyay, B. C. Mitra, D. Mondal, S. K. Ghosh, D. Chattopadhyay. (2018b). Jute cellulose nano-fibrils/hydroxypropylmethylcellulose nanocomposite: a novel material with potential for application in packaging and transdermal drug delivery system. *Industrial Crops and Products*, 112, 633-643. [CrossRef]
9. N. Mao, S. J. Russell. Capillary pressure and liquid wicking in three-dimensional nonwovenmaterials. *Journal of Applied Physics*, 104, 034911 (2008). [CrossRef]
10. AS 2836.4-1998 Methods of Testing Surgical Dressings & Surgical Dressing Materials– Method for the Determination of Size.
11. P. W. Chuleigh. (1983). Image formation by fibres and fibre assemblies, *Textile Research Journal*, 54, 813. [CrossRef]
12. R. Chhabra. (2003). Nonwoven Uniformity – Measurements Using Image Analysis, *International Nonwovens Journal*, 12(1), 43–50. [CrossRef]
13. J. W. S. Hearle, P. J. Stevenson. (1963). Nonwoven fabric studies, part 3: The anisotropy of nonwoven fabrics. *Textile Research Journal*, 33, 877–888. [CrossRef]
14. D. P. Dubrovski, M. Brezocnik. (2016). Porosity and nonwoven fabric vertical wicking rate. *Fibers and Polymers*, 17(5), 801–808. DOI:10.1007/s12221-016-6347-5. [CrossRef]
15. H. H. Epps, K. K. Leonas. (2000). Pore Size and Air Permeability of Four Nonwoven Fabrics. *International Nonwovens Journal*, os-9, 2. https://doi.org/10.1177/1558925000OS-900215. [CrossRef]
16. E. Çinçik, E. Koç. (2011). An analysis on air permeability of polyester/viscose blended needle-punched nonwovens. *Textile Research Journal*, 82(5), 430–442. [CrossRef]

17. N. Gobi, S. Evangelin, R. Kasthuri, D. Nivetha. (2019). Multilayer nonwoven fabrics for filtration of micronand submicron particles. *Journal of Textile Engineering and Fashion Technology*, 5(2):81–84. [CrossRef]
18. P. Soltani, M. S. Johari, M. Zarrebini. (2015). 3D Fiber Orientation Characterization of Nonwoven Fabrics using X-ray Micro-computed Tomography. *World Journal of Textile Engineering and Technology*, 1, 41-47.
19. E. M. Yüksekkaya, M. Tercan, G. Doğan, (2010). Filter media research: Fabric reinforcement of nonwoven filter cloths. *Filtration & Separation*, 47(3), 36–39. [CrossRef]
20. M. T. Wright, M. C. Carr, A. C. Grant, V. Lilladhar, J. S. Russell. (2015). Strength of hydroentangled fabrics manufactured from photo-irradiated poly para-phenyleneterephthalamide (PPTA) fibres. *Polymer Degradation and Stability*, 121, 193–199. doi:10.1016/j.polymdegradstab.2015.08.017[CrossRef]
21. P. K. Patnaik, R. T. P. Swain, K. S. Mishra, A Purohit, S. Biswas. (2020). Recent developments on characterization of needle-punched nonwoven fabric reinforced polymer composites – A review. Materials Today: Proceedings. DOI:10.1016/j.matpr.2019.12.086[CrossRef]
22. J-H. Li, C-J. Hsieh, W-C. Lou, T-C. Hsieh, J-Y. Pan, Y.-J., Hsing, W.-H., H-J. Lin. (2016). Needle-punched thermally-bonded eco-friendly nonwoven geotextiles: Functional properties. *Materials Letters*, 183, 77–80. DOI:10.1016/j.matlet.2016.07.074[CrossRef]
23. H. H. Epps, K. K. Leonas. (2002). GA. Pore Size and Air Permeability of Four Nonwoven Fabrics. DOI: https://journals.sagepub.com/doi/pdf/10.1177/1558925000OS-900215
24. A. Zaman, J. T. Orasugh, P. Banerjee, S. Dutta, M. S. Ali, D. Das, A. Bhattacharya, D. Chattopadhyay. (2020). Facile one-pot in-situ synthesis of novel graphene oxide-cellulose nanocomposite for enhanced azo dye adsorption at optimized conditions. *Carbohydrate Polymers*, 2020, 116661. [CrossRef]
25. ASTM D737-96 Test Method for Air Permeability of Textile Fabrics.
26. BS EN ISO 9237:1995 Textiles. Determination of the permeability of fabrics to air; ISO/DIS 9073-15: 2005 Textiles – Test methods for nonwovens – Part 15: Evaluation of air permeability.

AUTHORS PROFILE

Dr. Jonathan Tersur Orasugh, is a currently a postdoctoral researcher with the Department of Chemical Sciences, University of Johannesburg, Doorfontein, Johannesburg 2028, South Africa.

Dr. Kausik Bal, is currently the development and Planning Officer, University of Calcutta, Kolkata, West Bengal, India. He is also a lecturer with the Department of Jute and Fibre Technology, Institute of Jute Technology, University of Calcutta, 35 Ballygunge Circular Road, Kolkata -700 019, West Bengal, India.

Prof. (Dr.) Dipankar Chattopadhyay, is the former head of department and Professor with Department of Polymer Science and Technology, University of Calcutta, 92 A.P.C. Road, Kolkata -700 009, India. He is experienced, resourceful and well-published teaching and research professional with expertise in Polymer Science and Technology: synthesis and characterization, polymer nanocomposites, hydrogel-based biomaterial, rubber compounding and technology, conducting polymers and initiative to affect creative solutions to a broad range of research problems in the above fields. Experienced and knowledgeable research professional in the area of development of advanced polymers and nanomaterials with special emphasis on biodegradable, biocompatible advanced polymers and nanomaterials obtained through the dictates of green chemistry and green technology to meet the challenges of today's society.

Prof. (Dr.) Swapan Kumar Ghosh, is the former head of department and Professor with the Department of Jute and Fibre Technology, Institute of Jute Technology, University of Calcutta, 35 Ballygunge Circular Road, Kolkata -700 019, West Bengal, India. He is an active teaching Prof and also active research-wise. He is experienced, resourceful, and well-published teaching and research professional with expertise in Textile Technology, Polymer Science and Technology: synthesis and characterization, polymer nanocomposites, hydrogel-based biomaterial, rubber compounding and technology, geotextiles/geosynthetics, and initiative to affect creative solutions to a broad range of research problems in the above fields. Experienced and knowledgeable research professional in the area of development of advanced polymers and nanomaterials with special emphasis on biodegradable, biocompatible advanced polymers and nanomaterials to meet the challenges of today's society.

Professor Suprakas Sinha Ray is a Chief Researcher at the Council for Scientific and Industrial Research with a PhD in Physical Chemistry from the University of Calcutta in 2001, Manager of the Centre for Nanostructures and Advanced Materials and Director of the DSI-CSIR Nanotechnology Innovation Centre. He is also associated with the University of Johannesburg as a Distinguished Visiting Professor of Chemical Sciences. Ray's current research focuses on polymer-based advanced nanostructured materials and their applications.